

Confinement in 3D polynomial oscillators through a generalized pseudospectral method

Amlan K. Roy*

*Division of Chemical Sciences, Indian Institute of Science Education and Research Kolkata,
Mohanpur Campus, Nadia, 741252, India*

Abstract

Spherical confinement in 3D harmonic, quartic and other higher oscillators of even order is studied. The generalized pseudospectral method is employed for accurate solution of relevant Schrödinger equation in an *optimum, non-uniform* radial grid. Eigenvalues, eigenfunctions, position expectation values, radial densities in *low and high-lying* states are presented in case of *small, intermediate and large* confinement radius. The *degeneracy breaking* in confined situation as well as correlation in its *energy ordering* with respect to the respective unconfined counterpart is discussed. For all instances, current results agree excellently with best available literature results. Many new states are reported here for first time. In essence, a simple, efficient method is provided for accurate solution of 3D polynomial potentials enclosed within spherical impenetrable walls.

Keywords: Spherical confinement, polynomial oscillator, confined harmonic oscillator, degeneracy breaking, free harmonic oscillator, generalized pseudospectral method.

*Email: akroy@iiserkol.ac.in, akroy6k@gmail.com, Ph: +91-3473-279137, Fax: +91-33-25873020.

I. INTRODUCTION

Ever since the study of hydrogen atom inside an impenetrable spherical enclosure [1], confinement of quantum systems has witnessed many burgeoning activity in past few decades. This work was motivated by an attempt to understand effects of extreme pressure on electronic states. In such extremely small spatial dimensions, many fascinating phenomena occur in a quantum confined system, relative to the respective free system. Some of these relate to, e.g., thermodynamic properties in non-ideal gases, anharmonic effects in solids, impurity binding in quantum wells, partially ionized plasmas, mesoscopic scale artificial structures, etc. Gradually their importance was realized in various potential applications in physics and chemistry, such as quantum wells, quantum wires, quantum dots, etc. They have also relevance in the development of numerous nano-sized circuits including quantum computers. Usually, their unique physical, chemical properties are attributed to complex energy changes associated with them. Most widely studied quantum systems are particle in a box, harmonic oscillator, H atom, He and other many-electron atoms, as well as H_2^+ , H_2 and other molecules. The literature is vast; here we mention a few representatives [2–9].

Confinement problem in 1D confined harmonic oscillator (CHO) has been theoretically investigated by a number of workers over a long period of time [10–18]. For example, the effect of finite boundaries on a 1D CHO inside a potential enclosure was studied by means of WKB method [10]. Perturbative, asymptotic and Padé approximant solutions for boxed-in harmonic and inverted oscillators were reported [11]. Eigenfunctions, eigenvalues in such 1D potentials were also obtained by means of a hypervirial method [12, 13]. Accurate energies of 1D polynomial potentials having single and multiple wells inside a box were calculated through a Rayleigh-Ritz variation method by using a basis set of trigonometric functions [14]. A robust, strongly convergent numerical method has been proposed for harmonic, quartic and sextic oscillators [15]. Also, the trapped harmonic and quartic oscillators have been studied by a WKB method with appropriate boundary condition [16]. This employed a modified airy function method that ultimately leads to a modified Bohr-Sommerfeld-type quantization rule. Eigenvalues, dipole moments, Einstein coefficients of CHO have been considered by perturbation method [17] as well. Symmetric and asymmetric confinement was studied in [18] by a power series expansion and numerical method.

In parallel to the 1D problem mentioned above, some attention was been paid for simi-

lar studies in 2D, 3D and higher dimension, however with lesser intensity [19–33]. Several unique phenomena occur in such systems, especially related to *simultaneous, incidental and interdimensional* degeneracy [27–31]. In one of the earliest studies a hypervirial treatment was suggested for multidimensional isotropic bounded oscillators, including 3D CHO [19]. The 2D and 3D CHOs enclosed in circular and spherical boxes were considered in [20] by a Rayleigh-Schrödinger perturbative expansion as well as Padé approximant solution. A variational method [21] was proposed where the trial function was constructed as a product of “free” solutions of corresponding Schrödinger equation. However, the first systematic and accurate ground, excited states of 3D CHO (in terms of energies, eigenfunctions, spatial expectation values) with respect to box size were obtained in variational calculation of [22]. Later, results were also obtained by a WKB method [25]. A super-symmetric method [26] also offered reasonably accurate results. The N -dimensional CHO enclosed in an impenetrable spherical cavity was also computed by searching for the roots of hypergeometric function ${}_1F_1(a, b, z)$ [29]. Later, high-precision energies for N -dimensional CHO were presented by exploiting certain properties of hypergeometric function within the MAPLE computer algebra system [32]. Very recently, a combination of WKB method and a proper quantization rule has been advocated for CHO energy levels [33]. Energy characteristics of a 2D isotropic CHO, enclosed in a symmetric box were followed through annihilation and creation operators coupled with the infinitesimal operators of $SU(2)$ group [31]. Likewise, characteristic features in energy spectrum of 3D CHO were established by invoking analytical properties of Bessel and confluent hypergeometric functions. However, the most extensively studied confined system is H atom. A vast amount of reference exists on the subject emphasizing different kinds of confinement and theoretical methods [34–37].

In present communication, we are interested in the confinement studies in 3D quantum polynomial oscillators. It may be noted that while all these above methods produce reasonably good-quality results, only two [22, 32] of these offer energies with ten or higher significant figure accuracy for 3D oscillators. Moreover, there is a lack of good results in the *low radius of confinement*, and *higher excited states*. Further, while a substantial amount of accurate results exist for enclosed H atom problem, same for 3D CHO is much less and almost none for other polynomial potentials. We will use the generalized pseudospectral (GPS) method for this purpose, which in recent years, has been successfully applied to a wide range of *unconfined* physical and chemical systems. Some of these are spiked harmonic

oscillator, Hulthén, Yukawa, logarithmic, rational, power-law potentials, ro-vibrational levels in molecules as well as ground and Rydberg states in atoms, etc. [27, 38–43]. Only in [27], however, this was employed for confined quantum states. There, a few low-lying states such as $1s, 2p, 1d$ of 3D CHO were examined; additionally some degeneracy conditions were established. However a detailed performance of the GPS method in case of *confined* systems has not been made so far. In this work, we want to test its validity and relevance in such a context, which could extend its domain of applicability to larger set of problems. To this end, eigenvalues, eigenfunctions, expectation values are reported for low, high states. A detailed variation of eigenvalues with box size is also presented. Correlation between energies in *free* and respective *confined* system is discussed. Further, a similar study is made on quartic oscillator, which was not done before. Finally we consider confinement in even-degree polynomial oscillators (up to 20) in terms of changes in ground-state energy with radius of confinement. Section II gives a brief outline of the method used. Results are discussed in section III. We conclude with a few remarks in section IV.

II. METHOD OF CALCULATION

The GPS method has been found to be very successful for various physical and chemical systems as evidenced by the following applications [27, 38–43]. Therefore here we highlight only the essential aspects. Unless otherwise mentioned, atomic unit is employed.

The single-particle, non-relativistic time-independent radial Schrödinger equation can be written in following form (the problem is separable in radial and angular variables),

$$\left[-\frac{1}{2} \frac{d^2}{dr^2} + \frac{\ell(\ell+1)}{2r^2} + v(r) + v_c(r) \right] \psi_{n,\ell}(r) = E_{n,\ell} \psi_{n,\ell}(r) \quad (1)$$

where $v(r)$ is a polynomial potential of degree $2K$ containing only the dominant term, i.e., $v(r) = \frac{1}{2}r^{2K}$. In this work we consider $K = 1, 2, 3, \dots, 10$, while n, ℓ signify usual radial and angular momentum quantum numbers respectively. Last term in square bracket represents the confinement potential (r_c is the radius of confining spherical box),

$$v_c(r) = \begin{cases} +\infty & r > r_c \\ 0, & r \leq r_c \end{cases} \quad (2)$$

This equation needs to be solved with Dirichlet boundary condition $\psi_{n,\ell}(0) = \psi_{n,\ell}(r_c) = 0$.

A very distinctive feature of this approach is that it allows one to work in a *nonuniform*, *optimal* spatial discretization; a coarser mesh at larger r and a denser mesh at smaller r , while maintaining similar accuracies at both regions. Thus, compared to many other methods, much smaller number of grid point often suffices to recover very good accuracy for low and high states.

At first, a function $f(x)$ defined in an interval $x \in [-1, 1]$ is approximated by an N -th order polynomial $f_N(x)$,

$$f(x) \cong f_N(x) = \sum_{j=0}^N f(x_j) g_j(x), \quad (3)$$

so that the approximation is *exact* at *collocation points* x_j , i.e., $f_N(x_j) = f(x_j)$. In the Legendre pseudospectral method used here, $x_0 = -1$, $x_N = 1$, while $x_j (j = 1, \dots, N-1)$ are obtained from roots of first derivative of Legendre polynomial $P_N(x)$ with respect to x , i.e., $P'_N(x_j) = 0$. Cardinal functions, $g_j(x)$ in Eq. (3) satisfy the relation, $g_j(x_{j'}) = \delta_{j'j}$. Next, one can map the semi-infinite domain $r \in [0, \infty]$ onto finite domain $x \in [-1, 1]$ by a transformation $r = r(x)$ and introduce a nonlinear algebraic mapping of following form,

$$r = r(x) = L \frac{1+x}{1-x+\alpha}, \quad (4)$$

where L and $\alpha = 2L/r_{max}$ are two adjustable mapping parameters. Now, introducing a transformation of the type $\psi(r(x)) = \sqrt{r'(x)}f(x)$, followed by a symmetrization procedure leads to a *symmetric* matrix eigenvalue problem which can be easily solved by standard available routines (NAG libraries used) to yield accurate eigenvalues and eigenfunctions.

Sample calculations were performed for a sufficiently large sets of mapping parameters to monitor the accuracy and reliability of present method, so as to produce “stable” results with respect to reference results. This lead to a choice of $\alpha = 25$, $N = 200$, which appeared to be satisfactory for the problem at hand. Results in various tables are reported only up to the precision that maintained stability and they are *truncated* rather than *rounded-off*. Thus, they may be considered as correct up to the decimal place given.

III. RESULTS AND DISCUSSION

At first, in Table I, we present first six eigenvalues corresponding to radial quantum numbers $n = 0$ and 1 having $\ell = 0, 1, 2$, of 3D isotropic CHO in a spherical box with impenetrable

TABLE I: Energies (a.u.) of 3D CHO for $n = \{0, 1\}; \ell = \{0, 1, 2\}$ states. PR means Present Result.

r_c	$E_{0,0}$ (PR)	$E_{0,0}$ (Literature)	$E_{0,1}$ (PR)	$E_{0,1}$ (Literature)
0.1	493.48163346	493.481632 ^{a, b}	1009.5383008	1009.538302 ^{a, b}
0.3	54.843855432	54.843855 ^{a, b}	112.18757119	112.187571 ^{a, b}
0.5	19.774534180	19.774534 ^{a, b, c} , 19.774534179 ^{d, e}	40.428276496	40.428277 ^{a, b} , 40.428276497 ^d , 40.428276496 ^e
1.0	5.0755820154	5.0755820 ^c , 5.0755820152 ^{d, e, f} , 4.98501 ^g	10.282256939	10.282256939 ^{d, e, f} , 10.13941 ^g
1.5	2.5049761786	2.502471 ^a , 2.504976 ^b , 2.5049761 ^c , 2.5049761785 ^{d, f} , 2.54357 ^g	4.9035904193	4.901782 ^a , 4.903590 ^b , 4.9035904194 ^{d, f} , 4.87758 ^g
2.0	1.7648164388	1.732515 ^a , 1.764816 ^b , 1.7648087 ^c , 1.7648164387 ^{d, e}	3.2469470987	3.224167 ^a , 3.246947 ^b , 3.2469470987 ^{d, e, f} , 3.31861 ^g
3.0	1.5060815273	1.544195 ^a , 1.506082 ^b , 1.5060815272 ^d	2.5312924665	2.688286 ^a , 2.531292 ^b , 2.5312924666 ^d
4.0	1.5000146030	1.504181 ^a , 1.5000015 ^b , 1.50000146030 ^d	2.5001437781	2.517144 ^a , 2.500144 ^b , 2.5001437781 ^d
5.0	1.5000000037	1.500581 ^a , 1.500000 ^b , 1.5000000036 ^{d, e}	2.5000000584	2.502500 ^a , 2.500000 ^b , 2.5000000584 ^{d, e}
6.0	1.5000000000	1.5000000000 ^d	2.5000000000	2.5000000000 ^d
	$E_{0,2}$ (PR)	$E_{0,2}$ (Literature)	$E_{1,0}$ (PR)	$E_{1,0}$ (Literature)
0.1	1660.8752892		1973.9224834	
0.3	184.56119633		219.33897241	
0.5	66.489756534	66.489756534 ^d	78.996921147	78.996921150 ^{d, e}
1.0	16.827777109	16.827777109 ^d	19.899696502	19.899696501 ^{d, e, f} , 19.78300 ^g
1.5	7.8717304875	7.8717304877 ^d	9.1354220880	9.1354220876 ^{d, f} , 9.10021 ^g
2.0	5.0100408655	5.0100408656 ^d	5.5846390792	5.5846390790 ^{d, e, f} , 5.59685 ^g
3.0	3.5982476989	3.5982476989 ^d	3.6642196451	3.6642196450 ^{d, f} , 4.01642 ^g
4.0	3.5008420737	3.5008420738 ^d	3.5016915386	3.5016915385 ^d
5.0	3.5000005566	3.5000005567 ^d	3.5000012215	3.5000012214 ^{d, e}
6.0	3.5000000000	3.5000000003 ^d	3.5000000001	3.5000000000 ^d
	$E_{1,1}$ (PR)	$E_{1,1}$ (Literature)	$E_{1,2}$ (PR)	$E_{1,2}$ (Literature)
0.1	2983.9775336		4135.9634334	
0.3	331.56849477		459.56818797	
0.5	119.40244526	119.40244525 ^d , 119.40244526 ^e	165.48541838	
1.0	30.013487593	30.013487592 ^d , 30.013487591 ^{e, f} , 29.88263 ^g	41.547472167	41.547472166 ^f , 41.40000 ^g
1.5	13.653740893	13.653740893 ^d , 13.653740892 ^f , 13.60644 ^g	18.805042927	18.805042927 ^f , 18.74733 ^g
2.0	8.1595288818	8.1595288816 ^{d, e, f} , 8.15237 ^g	11.093419194	11.093419194 ^f , 11.07445 ^g
3.0	4.9138976907	4.9138976907 ^{d, f} , 5.05725 ^g	6.3076308117	6.3076308118 ^f , 6.37769 ^g
4.0	4.5083304309	4.5083304308 ^d	5.5286815696	
5.0	4.5000105731	4.5000105730 ^{d, e}	5.5000647985	
6.0	4.5000000011	4.5000000008 ^d	5.5000000098	

^aRef. [20].

^bAs quoted in [20].

^cRef. [19].

^dRef. [22].

^eRef. [32].

^fAs quoted in [33].

^gRef. [33].

walls. Depending on the box size, confinement can be classified in three distinct regions, namely, *small*, *intermediate* and *large* r_c . Ten cage radii were chosen for this purpose. First definitive result of the lowest two states were presented through a Rayleigh-Schrödinger-type perturbation expansion having free-particle in a box as the unperturbed system [20]. They

TABLE II: Eigenvalues (in a.u.) of $n = 8, \ell = \{0 - 8\}$ states of 3D CHO as function of r_c .

ℓ	$r_c = 0.5$	$r_c = 1.5$	$r_c = 2.5$	$r_c = 3.5$	$r_c = 4.5$	$r_c = 10$
0	1598.9175016	178.02733028	64.998075416	34.693293571	23.225703703	17.500000000
1	1777.5046290	197.87206375	72.146061470	38.344628587	25.432849261	18.499999999
2	1961.9446659	218.36830761	79.531522574	42.122176083	27.724249606	19.499999999
3	2152.2122548	239.51291591	87.152525538	46.023630724	30.096639843	20.500000000
4	2348.2769485	261.30226934	95.007188871	50.047065889	32.547442956	21.500000000
5	2550.1056822	283.73252093	103.09370240	54.190838285	35.074586281	22.500000000
6	2757.6642785	306.79974464	111.41033572	58.453522134	37.676374299	23.499999999
7	2970.9183755	330.50002581	119.95544047	62.833862466	40.351398586	24.499999999
8	3189.8339986	354.82951614	128.72744924	67.330741133	43.098472783	25.499999999

also computed these states employing various Padé approximations. Here, we quote their $P[1/5]$ energies in third column, while perturbation energies are omitted to save space. Perturbation and Padé eigenvalues differ amongst each other significantly, especially when the system is enclosed in a larger box (larger r_c). Their numerical eigenvalues obtained by diagonalizing the Hamiltonian matrix in a basis of free particle-in-a-box eigenfunctions appear to be superior to above both, and referred here. While these are decent initial estimates, present GPS energies are significantly improved over these. Confinement in the intermediate region was studied for ground state by means of a hypervirial method [19]. In this case, the accuracy generally becomes less precise as r_c increases; for low r_c , these are more or less of similar quality as in [20]. Quite accurate eigenvalues for all states except $E_{1,2}$ (in the range $r_c > 0.5$) have been reported through variational procedure [22]. Here the two integers in subscript denote n, ℓ quantum numbers respectively. Current energies are in excellent agreement with these values for whole range of r_c ; in several occasions exactly reproducing those of the reference. However the most accurate energies are those published in [32]; these are obtained as roots of a transcendental equation written in terms of confluent hypergeometric functions. The authors used familiar MAPLE algebra program to achieve impressive (as high as up to 100-digit) accuracy in eigenvalues. These are available for $n = \ell = 0, 1$ states at selected r_c . Here also, the GPS results offer excellent agreement with these energies. Very recently some of these states are also calculated by a combination of quantization rule and WKB method [33]. These are also produced here for comparison. Obviously in all instances, isotropic free harmonic oscillator (FHO) energies are recovered as $r_c \rightarrow \infty$.

Next we proceed in Table II for sample results on high-lying states. In order to demon-

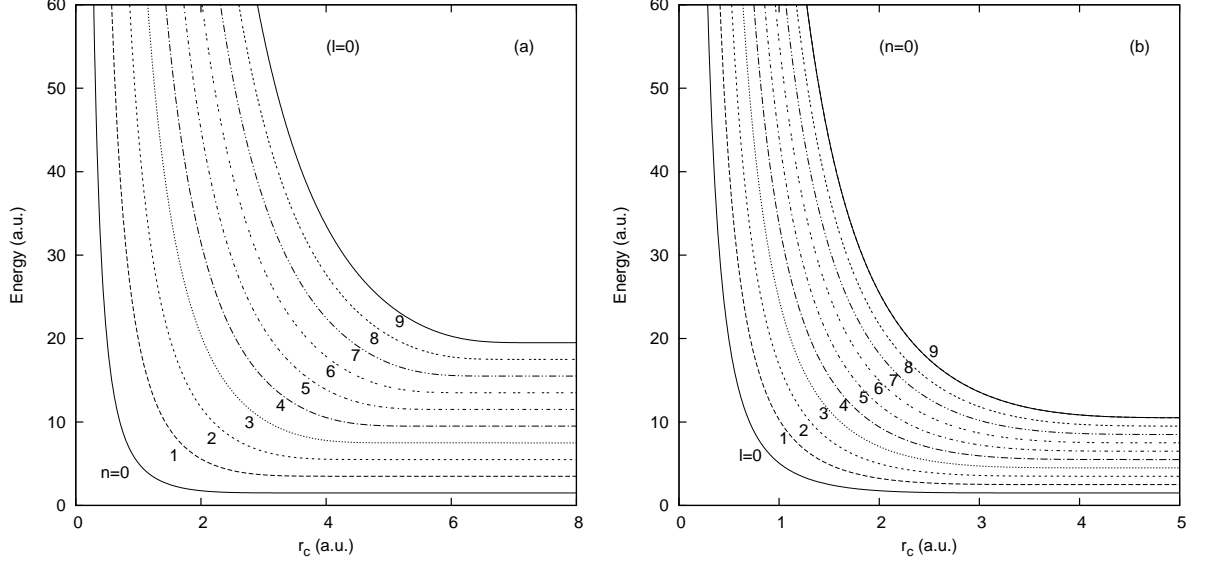


FIG. 1: Energy changes (a.u.) in 3D isotropic CHO for (a) $l = 0$; $n = 0 - 9$ and (b) $n = 0$; $l = 0 - 9$ levels respectively, as function of confining radius.

strate the viability and efficiency in such situations, nine states (having $\ell = 0 - 8$) corresponding to $n = 8$ are given. As in previous table, here again we cover the entire domain of confinement choosing six representative r_c values, *viz.*, 0.5, 1.5, 2.5, 3.5, 4.5 and 10 a.u. respectively. As evident from above discussion, while a decent number of high-quality references exist for confinement in low-lying states, there is a lack of such studies for higher excitations. Thus no literature values could be quoted for any of these. We hope that they would be helpful in future calibration of other methodologies. Once again, as box radius increases, energies of bounded system approach towards the 3D isotropic FHO eigenvalues.

Energy variations of Tables I, II are vividly depicted in Figure 1. The left panel (a) gives such plots for ten s -waves ($\ell = 0$) having radial quantum numbers $n = 0 - 9$, while in right panel (b), we consider same for ten lowest states (having $\ell = 0 - 9$ values) corresponding to the lowest n quantum number. Energy axes in both cases cover same range; whereas r_c axes differ in two occasions. In both cases, however, confinement in very small box radius is ignored to avoid high energy values, which makes these plots difficult to comprehend. To the best of our knowledge, such energy plots have been attempted before [32] only for ground state for a confinement region of $r_c = 0.5 - 3.5$ a.u. Present plots significantly extend the radius of sphere, and also cover low, high excited states, corroborating the previous findings for ground state. In both panels, neighboring plots are parallel and remain well separated. Generally, at low r_c , energies assume high values, falling off sharply with an increase in r_c to

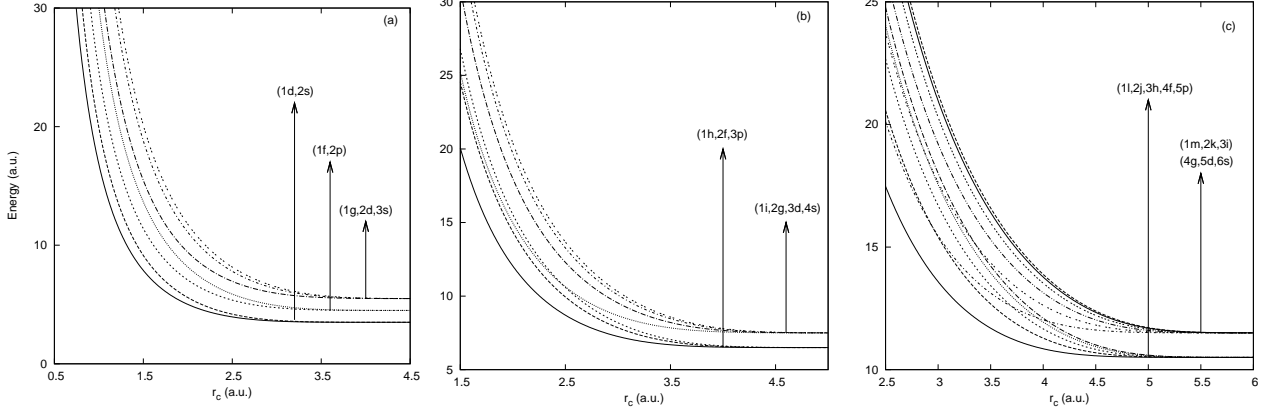


FIG. 2: Energy eigenvalues (a.u.) of (a) $(1d, 2s)$, $(1f, 2p)$, $(1g, 2d, 3s)$ (left), (b) $(1h, 2f, 3p)$, $(1i, 2g, 3d, 3s)$ (middle), and (c) $(1l, 2j, 3h, 4f, 5p)$, $(1m, 2k, 3i, 4g, 5d, 6s)$ (right) levels respectively, of 3D isotropic CHO as function of cavity radius.

approach the isotropic FHO results and finally becomes constant after attaining those. This is in keeping with the fact that energy of a confining system possessing spherical symmetry is a decreasing monotonic function of confining radius and as r_c is increased energy levels smoothly converge to the corresponding free system energy levels [30].

At this stage, we discuss the correlation in energy between 3D isotropic CHO and its unconfined counterpart FHO. It is well known [44] that the 3D isotropic FHO energy levels, given by $E_{k,\ell} = (k + \ell + \frac{3}{2}) = (m + \frac{3}{2})$ a.u., are degenerate. Here k is zero or *even* positive integer, ℓ is zero or *any* positive integer, so that m can have *all* integral values, zero or positive. Thus ℓ, m quantum numbers have same parity. Interestingly, when the 3D isotropic FHO is confined inside a spherical box, not only this characteristic degeneracy removed, but also the equal energy separation between adjacent levels of 3D FHO disappears [22, 31]. In left panel (a) of Figure 2, is shown the degeneracy breaking of three lowest degenerate levels of isotropic 3D FHO in presence of confinement, *viz.*, $(1d, 2s)$, $(1f, 2p)$, $(1g, 2d, 3s)$ having degeneracies of 2, 2, 3 respectively. For smaller values of r_c , the spectrum is clearly non-degenerate; as the former gradually increased, energy differences become smaller and finally at sufficiently high r_c , the levels merge, making them degenerate. However, in all these three instances, the three degenerate levels remain well separated and do not mix with each other. In middle panel (b) is given the degeneracy breaking of two $(1h, 2f, 3p)$, $(1i, 2g, 3d, 3s)$ levels of FHO (both having degeneracy of 3) under the influence of confinement. In this case, one notices moderate mixing of $1i$ and $3p$ states. Such mixings also happen between $1h$

TABLE III: Selected expectation values (in a.u.) of some low-lying states of 3D isotropic CHO at various r_c values. Numbers in the parentheses denote literature results.

r_c	n	ℓ	$\langle r^{-2} \rangle$	$\langle r^{-1} \rangle$	$\langle r \rangle$	$\langle r^2 \rangle$
0.5	0	0	35.669782840	4.8770025194	0.24993143144	0.07063332532
			(35.670362626 ^a)	(4.8770025195 ^b)	(0.24993143143 ^b)	(0.07063332531 ^a)
	1	0	75.007610219(75.00992708 ^a)	6.2285137551	0.25002044046	0.08017671929(0.08017667193 ^a)
	0	1	15.604579050(15.604579051 ^a)	3.7023250014	0.29578935362	0.09362593573(0.09362593572 ^a)
	1	1	28.8493991749(28.8493991689 ^a)	4.6995657221	0.26969402489	0.08682928611(0.08682928612 ^a)
1.0	0	0	9.0239897183(9.0241006941 ^a)	2.4512273473	0.49781081198	0.28044919195(0.2804491919 ^a)
	1	0	18.773367559(18.773803815 ^a)	3.1127583237	0.50064924778	0.32128003811(0.3212800381 ^a)
	0	1	3.9247112833(3.9247112835 ^a)	1.8561980355	0.59025087969	0.37296446428(0.3729644642 ^a)
	1	1	7.2212001400(7.2212001399 ^a)	2.3501690242	0.53961515964	0.34762136892(0.3476213689 ^a)

^aRef. [22].

^bRef. [32].

and $3s$ states (not shown). Finally, in right panel (c) such crossings are shown between the first penta-degenerate $(1l, 2j, 3h, 4f, 5p)$ and hexa-degenerate $(1m, 2k, 3i, 4g, 5d, 6s)$ levels respectively of the FHO. It has been pointed out that, when energy levels are functions of radius of confinement, it may so happen that, for some particular values of r_c , energies of two 3D CHO states coincide. This has been termed as *accidental degeneracy* in the sense it is defined in [30, 45]. The above mixing characteristics are manifestations of such intersections which happens for $(1h, 3s)$, $(1i, 3p)$, $(1j, 4s)$, $(1j, 3d)$, $(1j, 2g)$ pairs. The second one can be seen from (b), while in (c) several such cases appear. Clearly one encounters many complex splitting of energy levels for high n, ℓ quantum numbers as the box radius is decreased. In all these plots, as in Figure 1, energies in low- r_c region is omitted for ease of appreciation.

Energy orderings in 3D isotropic CHO states in the limit of $r_c \rightarrow \infty$ is found to be,

$$1s, 1p, (1d, 2s), (1f, 2p), (1g, 2d, 3s), (1h, 2f, 3p), (1i, 2g, 3d, 4s), (1j, 2h, 3f, 4p), \\ (1k, 2i, 3g, 4d, 5s), (1l, 2j, 3h, 4f, 5p), (1m, 2k, 3i, 4g, 5d, 6s), \dots$$

For convenience, the degenerate states are grouped in parentheses. Such orderings up to $4s$ were noticed in the variational calculation of [22] and up to $1j$ in [30] from the zeros of Bessel functions. Our calculation reproduces these two previous works and present an extended ordering of levels. In the limit of $r_c \rightarrow 0$, the same changes to,

$$1s, 1p, 1d, 2s, 1f, 2p, 1g, 2d, 1h, 3s, 2f, 1i, 3p, 1j, 2g, 3d, 4s, 1k, 2h, 3f, 1l, 4p, 2i, \dots$$

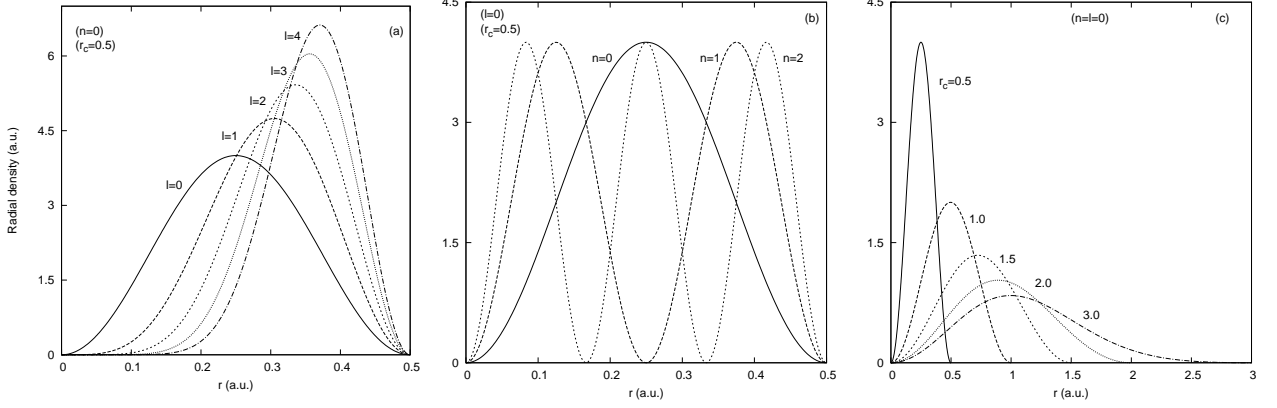


FIG. 3: Radial distribution functions (a.u.) of 3D isotropic CHO: (a) $n = 0; l = 0 - 4$ states for $r_c = 0.5$; (b) $l = 0; n = 0 - 2$ states for $r_c = 0.5$; (c) ground state for $r_c = 0.5, 1.0, 1.5, 2.0, 3.0$.

In this case also, the relative ordering of first 13 states given in [22] and 17 states considered in [30] are the same as found here, although we have covered some higher states.

As a further proof of the usefulness of present work, Table III reports four position expectation values, *viz.*, $\langle r^{-2} \rangle$, $\langle r^{-1} \rangle$, $\langle r \rangle$, $\langle r^2 \rangle$ of 3D isotropic CHO under the spherical confinement. Two lowest n states (0 and 1) corresponding to two lowest ℓ values of 0 and 1 are given for two r_c (0.5, 1). The first and last expectation values for all the states were earlier reported quite accurately in [22]. Our results show very good agreement with these reference values, which is apparently better for latter than the former. The other two expectation values, $\langle r^{-1} \rangle$, $\langle r \rangle$ are available only for ground state having an $r_c = 0.5$. Once again, GPS values are in excellent agreement with the literature values. No reference results could be found for these two expectation values for remaining 7 states.

Now, Fig. 3 depicts some sample radial density distribution functions in case of isotropic bounded HO. In left panel (a), we show such plots for 5 lowest $n = 0$ states having l values 0–4 confined in a box of radius $r_c = 0.5$. As l increases, the peak height increases, shifts to the right side and tends to become more compact. The middle panel (b) displays density plots for 3 lowest states (having $n = 0 - 2$) corresponding to $l = 0$ for same fixed r_c as in (a). With an increase in n , one notices an increase in the number of nodes, whereas the maxima in density peaks remain practically unchanged. Finally (c) shows density changes in ground state of 3D CHO for five values of box radii, *viz.*, 0.5, 1.0, 1.5, 2.0 and 3.0 covering a decent range of confinement. With increase in r_c , density peaks reduce to smaller values and tend to spread, eventually assuming the shape of that of an FHO for sufficiently large

TABLE IV: Lowest six eigenvalues (in a.u.) of 3D confined isotropic quartic oscillator at selected r_c values. Ground-state energy of the free oscillator is 1.8998365149 a.u. [24].

r_c	$E_{0,0}$	$E_{0,1}$	$E_{0,2}$	$E_{1,0}$	$E_{0,3}$	$E_{1,1}$
0.1	493.48022579	1009.5364365	1660.8731068	1973.9208888	2441.5596954	2983.9758067
0.3	54.831597579	112.17141900	184.54236135	219.32525354	271.28548566	331.55364336
0.5	19.742773482	40.386895144	66.441916477	78.962323706	97.670693709	119.36502732
0.8	7.7339639376	15.809618718	25.996944579	30.878482788	38.203785113	46.663916029
1.0	4.9915845102	10.182113375	16.720373986	19.827020261	24.548286154	29.935709434
1.3	3.0794268551	6.2185008173	10.143870741	11.930708685	14.823708103	17.930956677
1.5	2.4678149050	4.9124620930	7.9342161030	9.2167903356	11.511774354	13.748897606
2.0	1.9412531888	3.6821177561	5.7125440986	6.2917841210	8.0174364761	8.9903956010
2.5	1.9002398159	3.5559309679	5.4265578434	5.8330487239	7.4754923256	8.0492393137
3.0	1.8998367875	3.5542235225	5.4212247115	5.8223857288	7.4617247879	8.0163868627
5.0	1.8998365150	3.5542220840	5.4212190000	5.8223727555	7.4617057604	8.0163311984

r_c . Number of nodes of a state remains same for all values of r_c .

Next we consider confinement in case of an isotropic 3D quartic harmonic oscillator. Six lowest eigenstates of this system are tabulated in Table IV for various box radii r_c . Here too a broad range of r_c is considered. To the best of our knowledge, such confinement studies have not been presented before. However, some eigenstates in free system have been reported in [24], where extremely accurate energies were obtained by expanding the wave function in a Fourier-Bessel series. Our ground-state energy of 1.8998365150 a.u. at last r_c is in very good agreement with their estimated value of 1.89988365149 a.u. Note that in this case, the critical boundary parameter L_{cr} , according to [24] is 4.75. This is defined as the value of the boundary length for which $E(L_{cr}) - E(L_{cr} + \delta)$ remains below a certain predefined small value (they fixed at 10^{-30}), for all values of $\delta > 0$. The energy orderings (both unconfined and confined) in this case also follow same sequence as found for 3D isotropic harmonic oscillator (this is confirmed for all the states given for harmonic oscillator). Of course, in the free quartic oscillator case, the degeneracies now disappear.

Now, Fig. 4 displays the above energy variations of 3D quartic isotropic oscillator with respect to changes in box radius. As in Fig. 1, here also, first ten $l = 0$ states corresponding to $n = 0 - 9$ are shown in left panel (a), whereas the right panel (b) considers first ten $n = 0$ states with angular quantum number 0–9. The r_c axis is kept fixed in both cases, while energy axis differs. Very small confinements are again omitted for easy appreciation of the plots. Qualitatively speaking the general trend remains very similar to those in Fig. 1 for

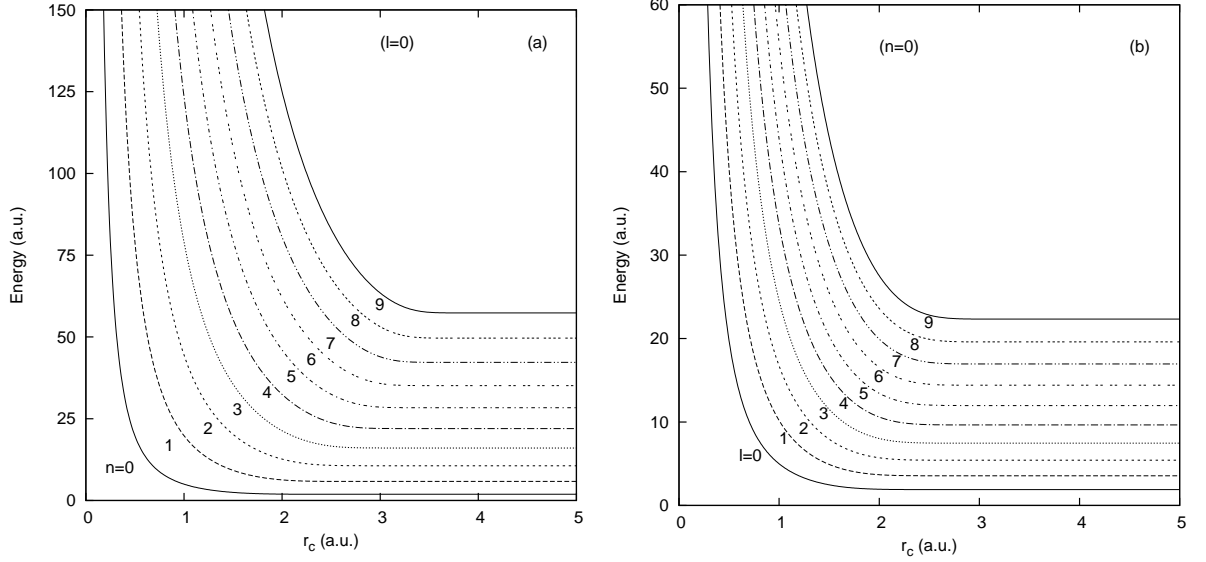


FIG. 4: Energy changes of 3D confined quartic HO potential for (a) $l = 0; n = 0 - 9$ and (b) $n = 0; l = 0 - 9$ levels respectively, as function of confinement radius r_c , in a.u.

3D CHO. Adjacent curves remain well-separated and parallel in both occasions. Energies tend to fall off sharply with an increase in r_c at the beginning; then becomes stationary after reaching the value of that of the respective 3D unconfined oscillator. One finds that, free unconfined oscillator energies are attained for relatively smaller values of r_c in this case, compared to the same in CHO. Such plots are given here for first time.

Next we shift our focus on confinement studies in 3D polynomial potentials of higher degree, namely $2K$, with $K = 3 - 10$. At first, however, Table V provides six eigenstates of respective free oscillators corresponding to n, ℓ quantum numbers (0,5) and (0,5,10) respectively, i.e., (0,0), (0,5), (0,10), (5,0), (5,5), (5,10) states. In this case, literature data is rather scanty; we could find only a lone reference of [24]. The authors reported first five of above states of anharmonic oscillators having $K = 3, 4, 10$. In all occasions, GPS results are identical to reference energies except for lowest state, where they differ from each other by only 2×10^{-10} a.u. This clearly demonstrates the validity and efficiency of current approach.

Finally, we present results of spherical confinement in some high, even-order isotropic 3D anharmonic oscillators. Ground states of six such polynomial oscillators having $2K = 6, 8, 10, 12, 16$ and 20 are offered in Table VI, varying the box radius from small to larger values. We are not aware of any such confinement studies before; hence no reference values could be quoted for direct comparison. However, the lowest states of free anharmonic oscillators having $2K$ values 6,8 and 20 were estimated earlier [24]. Our GPS energies in

TABLE V: Some low- and high-lying eigenvalues (in a.u.) of unconfined 3D polynomial potentials of even degree ($2K$). Literature values in parentheses are quoted from [24].

K	$E_{0,0}$	$E_{0,5}$	$E_{0,10}$	$E_{5,0}$	$E_{5,5}$	$E_{5,10}$
3	2.1692993559 (2.1692993557)	15.859640450 (15.859640450)	36.010035895 (36.010035895)	44.196187884 (44.196187884)	74.182455900 (74.182455900)	107.23827462
4	2.3779372071 (2.3779372069)	18.693357492 (18.693357492)	44.256045884 (44.256045884)	57.560400554 (57.560400554)	99.689155552 (99.689155552)	147.06867947
5	2.5489382648	20.856314303	50.629764312	68.606297125	121.31727693	181.41445326
6	2.6934707830	22.574874381	55.691777381	77.756594924	139.54557480	210.69341741
7	2.8180925155	23.984159530	59.816772453	85.407643316	154.97516807	235.68085749
8	2.9271124526	25.168625012	63.253598497	91.876672206	168.13894256	257.12973408
9	3.0235635760	26.183608461	66.170973123	97.407233060	179.46908706	275.67781244
10	3.1096802645 (3.1096802643)	27.066934477 (27.066934477)	68.686384500 (68.686384500)	102.18488145 (102.18488145)	189.30659360 (189.30659360)	291.84162253

these three occasions show very good agreement with these reference values. For lower r_c , energies seem to change rather slowly with increase in $2K$. The estimated values of critical boundaries $L_{cr} = 3.6, 2.9$ and 1.72 in these three states [24], decrease with the power and are well supported by energies given in this table. Considering the performance of our present approach in the context of various confinement situations discussed earlier, we are confident that these results of higher order polynomials would also be equally accurate and reliable. Although we have not ventured into estimating the L_{cr} , in general, however, the present calculation seems to corroborate the results of [24].

These above features of previous table are well reflected in Fig. 5, where energies of three low-lying states, namely, $(0,0)$, $(0,1)$ and $(1,0)$, of 3D spherically confined isotropic anharmonic oscillators of even orders $2, 4, 6, \dots, 20$ are plotted against the radius of confinement. Energy ranges are different in three plots while r_c axis remains same in (b), (c). From very close values at smaller r_c , individual energies decrease sharply and then assumes the constant value of corresponding unconfined potential, for critical values of the boundary parameter L_{cr} . As evident, in all these three occasions, L_{cr} decrease as $2K$ increase.

IV. CONCLUSION

A detailed analysis has been made to understand confinement in the family of 3D anharmonic oscillators of even order enclosed within spherically impenetrable walls. Energies,

TABLE VI: Ground-state energies (in a.u.) of some higher degree ($2K = 6, 8, 10, 12, 16, 20$) 3D polynomial oscillators enclosed within a spherical box of radius r_c a.u.

r_c	$K = 3^a$	$K = 4^a$	$K = 5$	$K = 6$	$K = 8$	$K = 10^a$
0.1	493.48022012	493.48022009	493.48022009	493.48022009	493.48022009	493.48022009
0.3	54.831156039	54.831136597	54.831135622	54.831135569	54.831135565	54.831135565
0.5	19.739647612	19.739270202	19.739218199	19.739210339	19.739208850	19.739208805
0.8	7.7179857725	7.7132646295	7.7116613437	7.7110607571	7.7107156751	7.7106485219
1.0	4.9627782237	4.9504713676	4.9443993675	4.9410809804	4.9378971947	4.9365423998
1.5	2.4843022335	2.5349157915	2.6136557597	2.7133768531	2.9275486225	3.1096805499
2.0	2.1713945253	2.3779504727	2.5489382668	2.6934707830	2.9271124526	3.1096802645
2.5	2.1692993821	2.3779372071	2.5489382648	2.6934707830	2.9271124526	3.1096802645
3.0	2.1692993559	2.3779372071	2.5489382648	2.6934707830	2.9271124526	3.1096802645
4.0	2.1692993559	2.3779372071	2.5489382648	2.6934707830	2.9271124526	3.1096802645

^a Energies at $r_c \rightarrow \infty$ for $K = 3, 4, 10$ respectively are: 2.1692993558, 2.3779372070 and 3.1096802643 a.u. [24].

expectation values, radial densities are obtained by means of GPS method. For isotropic 3D CHO, these quantities show excellent agreement with the best reference results available in literature, covering *small, intermediate and large* radius of confinement. It may be noted that, good-quality results in confined systems are obtainable by a number of attractive and elegant methodologies for *medium and large* r_c ; however, same for small r_c is rather scarce. In this work, we are able to generate quite good results in both these regions with equal ease and efficacy. Also, similar accuracy results are also offered in case of high-lying states. A thorough analysis of energy changes with respect to confinement radius has been made. Energy ordering in case of 3D CHO and free oscillator, as well as the degeneracy pattern is also discussed. Several interesting mixings have been pointed out. Next, we perform similar investigation on 3D quartic oscillator. Finally we briefly touch upon the case of 3D isotropic even-order isotropic bounded oscillators for higher orders up to as high as 20. Once again, low- and high-lying states in the confined system and free oscillator are presented in some detail. Energy changes with variations in r_c are monitored for selected low-lying states in such oscillators. The method also delivers excellent quality results in case of unconfined oscillators. Comparison with literature data reveals very good agreement in case of small as well as large box sizes. Confinement studies in other physical and chemical situations such as the H atom or many-electron atoms may further consolidate the success of this approach, some of which may be taken up in future works. Many new states are reported here for

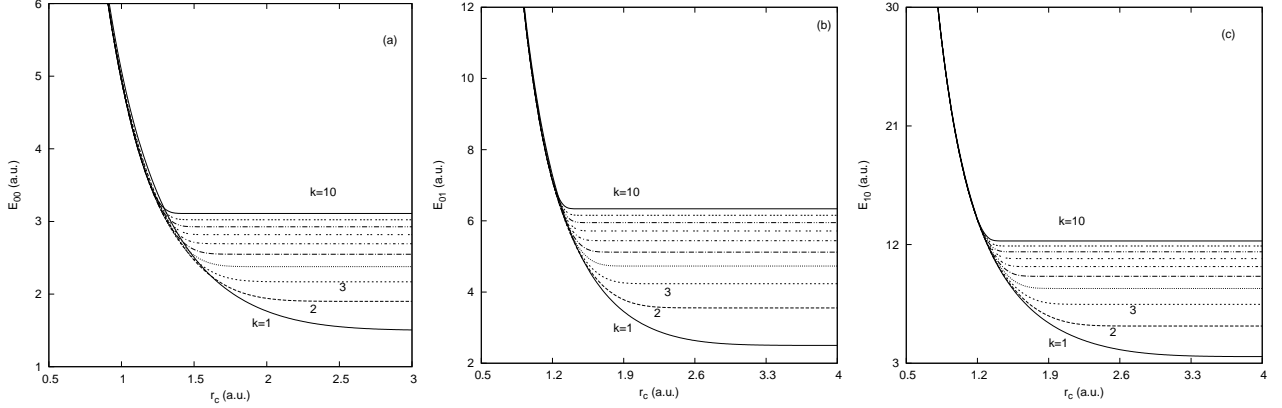


FIG. 5: Energies in spherically confined isotropic 3D even-order anharmonic oscillators ($2K = 2, 3, 4, \dots, 10$). Left, middle and right panels (a), (b), (c) correspond to $E_{0,0}$, $E_{0,1}$ and $E_{1,0}$ states with respect to box radius r_c , respectively. All quantities are in a.u. See text for details.

the first time. In summary, a simple, reliable method is offered for accurate calculation of harmonic and other higher order polynomial oscillators under spherical confinement.

-
- [1] A. Michels, J. De Boer and A. Bijli, *Physica* **4**, 981 (1937).
 - [2] P. W. Fowler, *Mol. Phys.* **53**, 865 (1984); *ibid.* **54**, 129 (1985).
 - [3] P. O. Fröman, S. Yngve and N. J. Fröman, *J. Math. Phys.* **28**, 1813 (1987).
 - [4] S. Yngve, *J. Math. Phys.* **29**, 931 (1988).
 - [5] W. Jaskólski, *Phys. Rep.* **271**, 1 (1996).
 - [6] J. P. Connerade, V. H. Dolmatov and P. A. Lakshmi, *J. Phys. B* **33**, 251 (2000).
 - [7] A. L. Buchachenko, *J. Phys. Chem. A* **105**, 5839 (2001).
 - [8] J. Gravesen, M. Willatzen and L. L. Y. Voon, *Phys. Scr.* **72**, 105 (2005).
 - [9] W. D. Heiss (Ed.) *Quantum Dots: A Doorway to Nanoscale Physics*, Springer, Berlin (2005).
 - [10] R. Vawter, *Phys. Rev.* **174**, 749 (1968).
 - [11] V. C. Aguilera-Navarro, E. Ley Koo and A. H. Zimmerman, *J. Phys. A* **13**, 3585 (1980).
 - [12] F. M. Fernández and E. A. Castro, *Int. J. Quant. Chem.* **20**, 623 (1981).
 - [13] G. A. Arteca, S. A. Maluendes, F. M. Fernández and E. A. Castro, *Int. J. Quant. Chem.* **24**, 169 (1983).
 - [14] H. Taşeli, *Int. J. Quant. Chem.* **46**, 319 (1993).
 - [15] R. Vargas, J. Garza and A. Vela, *Phys. Rev. E* **53**, 1954 (1996).

- [16] A. Sinha and R. Roychoudhury, *Int. J. Quant. Chem.* **73**, 497 (1999).
- [17] N. Aquino, E. Castaño, G. Campoy and V. Granados, *Eur. J. Phys.* **22**, 645 (2001).
- [18] G. Campoy, N. Aquino and V. D. Granados, *J. Phys. A* **35**, 4903 (2002).
- [19] F. M. Fernández and E. A. Castro, *Phys. Rev. A* **24**, 2883 (1981).
- [20] V. C. Aguilera-Navarro, J. F. Gomes, A. H. Zimerman and E. Ley-Koo, *J. Phys. A* **16**, 2943 (1983).
- [21] J. L. Marin and S. A. Cruz, *Am. J. Phys.* **59**, 931 (1991).
- [22] N. Aquino, *J. Phys. A* **30**, 2403 (1997).
- [23] H. Taşeli and A. Zafer, *Int. J. Quant. Chem.* **61**, 759 (1997).
- [24] H. Taşeli and A. Zafer, *Int. J. Quant. Chem.* **63**, 935 (1997).
- [25] A. Sinha, *J. Math. Chem.* **34**, 201 (2003).
- [26] E. D. Filho and R. M. Ricotta, *Phys. Lett. A* **320**, 95 (2003).
- [27] K. D. Sen and A. K. Roy, *Phys. Lett. A* **357**, 112 (2006).
- [28] H. E. Montgomery Jr. , N. Aquino and K. D. Sen, *Int. J. Quant. Chem.* **107**, 798 (2007).
- [29] S. M. Al-Jaber, *Int. J. Theor. Phys.* **47**, 1853 (2008).
- [30] Lj. Stevanović and K. D. Sen, *J. Phys. A* **41**, 225002 (2008).
- [31] Lj. Stevanović and K. D. Sen, *J. Phys. A* **41**, 265203 (2008).
- [32] H. E. Montgomery Jr. , G. Campoy and N. Aquino, *Phys. Scr.* **81**, 045010 (2010).
- [33] F. A. Serrano and S.-H. Dong, *Int. J. Quant. Chem.* **113** 2282 (2013).
- [34] N. Aquino, *Int. J. Quant. Chem.* **54**, 107 (1995).
- [35] B. L. Burrows and M. Cohen, *Int. J. Quant. Chem.* **106**, 478 (2006).
- [36] N. Aquino, G. Campoy and H. E. Montgomery Jr. *Int. J. Quant. Chem.* **107**, 1548 (2007).
- [37] H. Ciftci, R. L. Hall and N. Saad, *Int. J. Quant. Chem.* **109**, 931 (2009).
- [38] A. K. Roy, *J. Phys. G* **30**, 269 (2004).
- [39] A. K. Roy, *J. Phys. B* **37**, 4369 (2004); *ibid.* **38**, 1591 (2005).
- [40] A. K. Roy, *Phys. Lett. A* **321**, 231 (2004).
- [41] A. K. Roy, *Int. J. Quant. Chem.* **104**, 861 (2005), *ibid.* **113**, 1503 (2013), *ibid.* **114** 383 (2014).
- [42] A. K. Roy, *Pramana–J. Phys.* **65**, 01 (2005).
- [43] A. K. Roy, A. F. Jalbout and E. I. Proynov, *Int. J. Quant. Chem.* **108**, 827 (2008).
- [44] C. Cohen-Tannoudji, B. Diu and F. Laloë, *Quantum Mechanics*, Wiley-VCH, (1992).
- [45] J. P. Elliott and P. G. Dawber, *Symmetry in Physics*, London, Macmillan, (1979).